Separation Science and Technology
Publication details, including instructions for authors and subscription information:
http://www.informaworld.com/smpp/title~content=t713708471

Surfactant-Enhanced Electroosmotic Dewatering of Mineral Ultrafines

Christine S. Grant[ab]; Michael J. Matteson[a]; Eric J. Clayfield[a]
[a] School of Chemical Engineering, Georgia Institute of Technology, Atlanta, Georgia [b] Department of Chemical Engineering, North Carolina State University, Raleigh, North Carolina

To cite this Article Grant, Christine S. , Matteson, Michael J. and Clayfield, Eric J.(1991) 'Surfactant-Enhanced Electroosmotic Dewatering of Mineral Ultrafines', Separation Science and Technology, 26: 6, 773 — 802
To link to this Article: DOI: 10.1080/01496399108050496
URL: http://dx.doi.org/10.1080/01496399108050496

SEPARATION SCIENCE AND TECHNOLOGY, 26(6), pp. 773–802, 1991

Surfactant-Enhanced Electroosmotic Dewatering of Mineral Ultrafines

CHRISTINE S. GRANT,* MICHAEL J. MATTESON, and ERIC J. CLAYFIELD

SCHOOL OF CHEMICAL ENGINEERING
GEORGIA INSTITUTE OF TECHNOLOGY
ATLANTA, GEORGIA 30332

Abstract

The rate and extent of electroosmotic dewatering of mineral ultrafines are dependent on the surface charge density which is quantitatively measured by the zeta potential. This research tailors the surface electrical properties of a naturally uncharged ochre (iron oxide) mineral slurry by altering the concentration of potential determining hydroxide ions to facilitate electroosmotic dewatering. The adsorption of hydroxide ions (9×10^{-4} to 9×10^{-3} M) onto the iron oxide surface provides the necessary increase in zeta potential; however, the resulting electrostatic dispersion of the particles severely limits the hydraulic permeability. Subsequent addition of cetyl trimethyl ammonium bromide (5×10^{-4} to 5×10^{-3} M), a cationic surfacant, reflocculates the particles, while maintaining sufficient zeta potential to generate an electroosmotic effect. Hydraulic performance of the treated slurries is characterized by measurement of flow rate data and specific resistance determination. Further characterization of the electrokinetic properties through electrophoretic mobility studies verifies the proposed adsorption mechanism.

INTRODUCTION

The effective dewatering and separation of ultrafine particle dispersions is a critical problem area in mineral processing. As mineral ore grade decreases, more efficient separation techniques are necessary to isolate valuable material. This decrease in mineral grade results in the production of a large amount of mineral ultrafines. In industrial mineral processing, these ultrafines often constitute the premium product of the process. Fine particle dispersions, in the form of a tailing waste product, are also generated in the final steps of mineral processing, requiring adequate dewatering and disposal of these materials.

*To whom correspondence should be sent at her present address: Department of Chemical Engineering Box 7905, North Carolina State University, Raleigh, North Carolina 27695-7905.

The elements of concern in this study are as follows: 1) improvement of separation processing technology, 2) interfacial phenomena, and 3) rate and capacity of separations. The improvement of processing technology involves a change in separation strategies in addition to the incorporation of various driving forces (e.g., gravitational, electrical) and combinations of these forces in separation procedures. Specifically, the utilization of electrokinetic principles in conjunction with or as an alternative to hydraulic methods is explored.

The factor critically limiting conventional hydraulic dewatering methods is the solid particle size, which governs the filter cake pore size. When ultrafines are present, there is a considerable reduction in hydraulic permeability, which is a measure of the dewaterability of a system under the influence of a pressure gradient. In the case of ultrafines dewatering at the point where hydraulic separation becomes ineffective, thermal drying appears to be a viable alternative at this stage. However, it requires uneconomically large amounts of energy and may be unsuitable for heat-sensitive ultrafines. Another process for dewatering ultrafine slurries beyond the hydraulic limit is electrokinetic separation which uses electrical energy. A major advantage is that electrokinetic dewatering, in principle, is independent of particle size.

Electrokinetic phenomena pertain to the flow of a liquid that occurs at the solid/liquid interface under the influence of an applied potential gradient. Electroosmosis occurs when an external electric field is tangentially applied to a fixed surface, causing the mobile portion of the double layer to flow. The applied field induces the movement of excess counterions along the oppositely charged along with them, resulting in net liquid flow.

Recent examination of electrokinetic dewatering and thickening applications in current industries has been done by Sunderland (*1*). Previous work by Lockhart and others (*2*) has indicated that electrokinetic dewatering techniques can be effectively applied to fine particle systems. Research on the use of electrokinetic dewatering has been conducted on densification of large lagoons of metal mine tailings (*3*), coal ultrafines separation (*4*), and dewatering sludge from sewage treatment plants (*5–7*). The continuous separation of fine particles from high value product streams for more efficient transport and/or processing is the focus of the majority of electrokinetic separations research. However, the approach used by many researchers is largely empirical in that some fundamental parameters influencing electrokinetic separations (e.g., particle electric potential, state of aggregation, and relative magnitude of surface charge) have remained unexplored.

Investigations into the application of electroosmotic dewatering to systems in the absence of a significant natural particle surface charge are

limited. The charge on the particles governs the double-layer properties which determine the type of electrostatic interactions between particles. The mode of chemical action is to alter the nature of the electrical double layer surrounding the particle. Flocculation or the state of aggregation of particles is also determined by the surface electrical properties through the mechanisms of attraction and repulsion. In this work the modification of surface electrical properties is achieved through the addition of chemicals in the form of NaOH and a cationic surfactant.

Thus, the purpose of this research work is to explore the concept of chemically enhanced electroosmotic solid–liquid separation of mineral ultrafines. The synergistic effect of a surface conditioning agent and a cationic surfactant in the enhancement of electroosmotic dewatering is investigated.

Combined Field Filtration

When electroosmotic dewatering is carried out in combination with vacuum filtration, the total or overall flow rate in the system can be represented as

$$Q_{tot} = Q_{eo} + Q_{vac} \tag{1}$$

where Q_{tot} is the total flow rate, Q_{eo} is the flow rate due to electroosmosis, and Q_{vac} is the hydraulic or vacuum contribution to the overall flow rate. Individual flow rates may be predicted theoretically as a function of experimentally measurable parameters. A quantitative relationship may be established between the electroosmotic velocity of flow, the zeta potential, and the externally applied electric field (*8*, *9*).

Principles of Surfactant Action

Surfactants are utilized in the control of both surface charge and the hydrophobic-hydrophilic nature of a surface. When surfactants are utilized to alter surface properties for electroosmotic applications, the effect of interparticle interactions and charge are key parameters. The balance between the hydrophilic and hydrophobic properties of a surfactant represents an important parameter in surface activity. In aqueous systems, there are two primary mechanisms of surfactant adsorption: hydrophobic interactions and ionic interactions. On nonpolar surfaces, adsorption occurs by van der Waals attraction of the nonpolar tails to the hydrophobic surface. This action causes the polar hydrophilic group to become orientated toward the aqueous phase. The hydrophobic tail displaces water from the solid surface in an effort to become removed from the aqueous phase.

Hydrophilic surface adsorption occurs primarily by electrostatic interactions between the polar head group and the oppositely charged surface groups. In this case the surfactant molecule will become oriented with its hydrophobic groups toward the aqueous phase, causing the surface to become less readily wetted. Upon saturation of the sites of the potential determining ions by the surfactant, there is the possibility of multilayer adsorption at higher surfactant concentrations. The second multilayer adsorbs through van der Waals attractive forces based on the need for the hydrophobic tails to be removed from the water. The particle surface reverts back to a hydrophilic surface, with the polar group orientated toward the bulk phase. There is also charge reversal associated with multilayer adsorption, causing a change in the electrokinetic behavior of the system (*10*).

EXPERIMENTAL MATERIALS AND PROCEDURES

The parameters that govern ultrafines hydraulic dewatering include the pressure drop across both the filter medium and the material to be dewatered, the degree or extent of particle aggregation (flocculation), and associated packing properties of the system. In electroosmotic dewatering of ultrafines, the effectiveness of liquid removal is primarily a function of the charge of the particles, which is indicated by the zeta potential at the electrical double-layer interface.

The experiments in this study are designed to gather information to adequately describe how the above parameters interact during combined hydraulic and electroosmotic dewatering. A variety of experimental techniques are employed to quantitatively and qualitatively develop and support a dewatering mechanism.

Ultrafine Material

The ultrafine material ultilized in this study was ochre, which is a combination of various naturally occurring inorganic iron oxides. Ochre is represented by the general chemical formula $Fe_2O_3 \cdot H_2O$, with associated water. A complex iron oxide, ochre is often represented as a mixture of the following primary minerals: goethite, $HFeO_3$; limonite, $HFeO_3 \cdot nH_2O$; and hematite, Fe_2O_3. Ochre may also contain $Fe_2O_3 \cdot H_2$ and hydrous iron oxides.

Ochre is used as a pigment in a variety of end products including paints and coatings, construction materials, industrial chemical and foundry uses, and colorants for glass, ceramics, plastics, and textiles (*11*). A relatively inexpensive pigment, ochre is often utilized as a filler for more expensive pigments. The ochre pigments have the advantages of being lightfast, non-

reactive with solvents, resistant to bases and acids, in addition to being insoluble in water.

Ochre slurry samples were provided by the New Riverside Ochre Company in Cartersville, Georgia; a full scale mining facility producing crude naturally occurring iron oxide pigments. At New Riverside the critical step in processing is removal of water from the ultrafine slurry; this operation is currently performed by using a rotary vacuum filter followed by thermal drying. The ochre slurry was collected prior to the industrial rotary vacuum filter and had a fractional moisture content of 0.61 based on weight. This slurry contained no chemical additives (dispersants or flocculants), and earlier analysis by New Riverside indicated an approximate mean particle size of 2.5 μm. The average pH of the natural ochre slurry was 6.9.

Chemical Additives

The cationic surfactant used in this work was cetyl trimethyl ammonium bromide (CTAB) from the Aldrich Chemical Company with a purity of 95%, with the remaining 5% consisting of a stearyl compound. Different molarity stock solutions were prepared by diluting the CTAB in distilled water. All distilled water used was from a Corning Mega-Pure System (MP-6A) distillation column. The use of distilled water eliminated the possible addition of ions from tap water which may affect the electrical double layer on the ochre. The solid surface conditioning agent used in this research was the base sodium hydroxide (NaOH); NaOH stock solutions were prepared by dissolving Fisher Scientific NaOH pellets in distilled water.

Experimental Arrangement

All vacuum and electroosmotic dewatering tests were performed in a bench-scale batch dewatering cell. The dewatering cell consisted of a hydrophobic polyurethane Buchner funnel with the following dimensions: outer diameter, 10.69 cm; inner diameter, 10.26 cm; depth, 5.0 cm. The filter medium was Whatman #1 filter paper (9 cm diameter) which was placed over the perforations in the cell and secured by a polyurethane ring. This ring aided in the prevention of slurry seeping around the filter paper edges. Based on its resistance to rust and ease of soldering, electrodes for the electroosmotic studies were fabricated from bronze mesh screening. The bottom electrode was 9 cm in diameter with a continuous cord of solder on the outer edges to prevent screen fraying and to ensure electrical contact. A coated wire was attached to the edge of the circular electrode for connection with the power source. The upper electrode had a similar design, with an additional piece of Plexiglas (outer diameter, 8.75 cm;

inner diameter, 6.87 cm; thickness, 1.25 cm) attached to it with epoxy in order to maintain electrode contact with the filter cake.

Prior to a dewatering test, the bottom electrode was placed on top of the filter paper ring with the wire running up the inside wall of the cell. The electrode fit securely into the cell, thus preventing short circuiting by contact with the upper electrode. During the filter-cake formation, the upper electrode was positioned on the partially dewatered filter cake to provide an electrical contact for the passage of current. The upper electrode area corresponded to the area of the bottom electrode in order to generate a "uniform" electric field. In order to maintain constant resistance to liquid flow, both electrodes were positioned in the cell during experiments with and without applied potential.

The filtrate collection reservoir was a modified 100 mL Pyrex glass graduated cylinder. In order to accommodate the rubber stopper connected to the bottom of the dewatering cell, the top portion of the cylinder was altered by annealing and expanding approximately 4 cm of glass to the glass cylinder.

In all experiments the power source was a VIZ Model WP-705 dc power supply with a voltage range of 0 to 50 V. Voltages in this range assisted in the maintenance of a low power requirement; the majority of previous electroosmotic dewatering research have been performed in a voltage range of 5 to 55 V (*2*, *3*, *6*). The VIZ power supply also functioned as a dual digital display voltmeter/ammeter with a current range of 0.0 to 2.0 A.

Hydraulic pressure for the vacuum dewatering phase was provided by a Spectrum Vacutrol Lab Regular vacuum pump with a range of 0 to 760 mmHg. At 230 mmHg, the vacuum flow rate is the same order of magnitude as the electroosmotic flow rate in this work. Tubing to the dewatering cell was thick-walled Tygon vacuum tubing, with additional clamps implemented to sustain a constant vacuum.

Experimental Procedure

The stock ochre slurry was continuously mixed with a Stedfast Model SL 600 Stirrer using a pitched blade impeller. About 150 mL of the well-mixed ochre slurry was then transferred to a 250-mL tared beaker. The initial slurry pH and sediment volume were also measured at this stage. Following these analytical tests, the initial weight of the slurry was recorded. The base and/or surfactant was combined with the slurry in the form of a prepared liquid stock solution. Differing volumetric addition necessitates the recalculation of the value of the initial fractional moisture content.

The slurry was evenly poured into the dewatering cell followed by the application of the vacuum, which was adjusted to the set value. In all tests

the measured vacuum range was from 220 to 240 mmHg, with an average value of 230 mmHg. The slurry was permitted to filter under constant vacuum to partially consolidate the ochre. The volume of filtrate collected was continuously recorded over a period of 30 to 50 min. When approximately 50 mL liquid had been collected, the upper electrode was positioned on the filter cake. In some instances the electrode was partially submerged in the slurry remaining on top of the cake.

After 20 min of hydraulic dewatering, when a good filter cake had been formed, a constant potential of 35 or 45 V was applied to the system electrodes. During the dewatering test, frequent measurements were taken of the voltage and current across the filter cake. All dewatering experiments were conducted at room temperature with the top of the cell open to atmospheric pressure. The majority of the tests were carried out with the bottom electrode acting as the cathode; a few tests were undertaken with the anode as the bottom electrode to verify the polarity conditions for the best electroosmotic effect.

When liquid drainage had ceased, both the vacuum and potential were turned off; this occurred after 30 to 50 minutes of total dewatering time. The filter cake and the filtrate were retained for further physical and chemical property analysis. Subsequent zeta potential measurements were performed on prepared filtrate/filter cake samples.

Measurement of Surface Electrical Properties

In this research, determination of the zeta potential is carried out with a Rank Particle Micro-Electrophoresis Apparatus Mark II. A dilute colloidal dispersion of the particles to be measured is placed in the transparent glass cylindrical cell (0.26 mm inner diameter). Platinum blacked electrodes are positioned in the cell in contact with the dispersion to apply an electric field across the cell and generate an electrophoretic effect.

The actual measurement of particle electrophoretic velocities is performed by timing individual particles over a calibrated distance. The particles are timed in alternate directions (e.g., electrode polarity is reversed) in order to reduce or negate the effect of drift in the dilute particle dispersion. An average of approximately 20 timings (10 in each direction) on different-sized particles is used to calculate the electrophoretic velocity. In this research the zeta potential is calculated by using the rationalized form of the Smoluchowski equation.

The dispersing medium was the filtrate from an actual dewatering test with the solid particles obtained from the resulting filter cake. A Fisher Model 300 Ultrasonic Dismembrator was employed to disperse the dilute mixture, using the micro tip probe at 35% power output for approximately

5 min. The dispersion was then transferred into the cylindrical cell by a glass pipet.

Fractional Moisture Content

The data obtained from the dewatering test were in the form of volume liquid collected as a function of time, with the total dewatering time measured starting when the desired value of the vacuum was attained. Volumetric data (milliliter units) was recorded in intervals ranging from 30 to 100 s; more frequent readings were taken during the initial stages of electroosmotic dewatering. The addition of sodium hydroxide and CTAB in liquid form results in a change of the initial slurry liquid content. In order to account for this variation, the volumetric data were normalized and presented in the form of fractional moisture content vs dewatering time plots. The final molarity of base or surfactant within a slurry was calculated based on the actual amount of liquid in the slurry and modified accordingly.

t_{mod}

The total dewatering time is measured from the beginning of a test, and it incorporates both the vacuum and electroosmotic portion of the test. Separation of the electroosmotic and the hydraulic dewatering driving forces necessitates the development of a new time parameter, t_{mod}. t_{mod} is equal to zero at the point of potential application. In most instances t_{mod} is zero at a value of the total dewatering time (t) equal to 20 min.

RESULTS

Tests on Untreated Slurry

Plain test is a term used to describe the experiments conducted on the untreated slurry as received from the processing facility. Preliminary characterization of this slurry indicates to what extent the system must be chemically modified to facilitate an electroosmotic separation. The slurry sample in the current research was obtained from the New Riverside processing facility at various times. Although there was not a large variation in the hydrophobicity and the charge of the particles, there was a slight difference in the state of aggregation. For each slurry sample obtained, an initial series of dewatering tests were conducted to evaluate the reproducibility of the dewatering technique. Periodic checks of untreated slurry dewatering behavior were performed in between the chemical additive tests as a check with the initial experimental data.

Subsequent dewatering experiments were performed to determine whether the natural ochre particles had a sufficient zeta potential to create

an electroosmotic enhancement. A direct current of 35 V, with the cathode acting as the lower electrode, was applied to the filter cake; the results of this condition are indicated in Fig. 1. The lack of a marked variation in the slope of the curve upon application of a potential indicates there is not a significant electroosmotic enhancement in the dewatering rate. A reversal of the electrode polarity (bottom electrode as anode) yields a similar result, indicating the need for generation of charge at the surface.

The question of charge on the particle, or in this instance, the absence of charge, is verified by the zeta-potential measurements. When the electrophoretic mobility of the plain slurry was measured at varying applied potential and currents, no particle movement was observed corresponding to an electrophoretic mobility of zero (zeta potential necessarily zero also). These findings confirm the postulation that the particles are neutral in charge; it also establishes that the natural slurry is at the point of zero charge. The literature value of the point of zero charge for goethite is at a pH of 6.7 (*12*). In this research the measured pH of the untreated slurry is 6.3, which is in close proximity to the literature value for goethite.

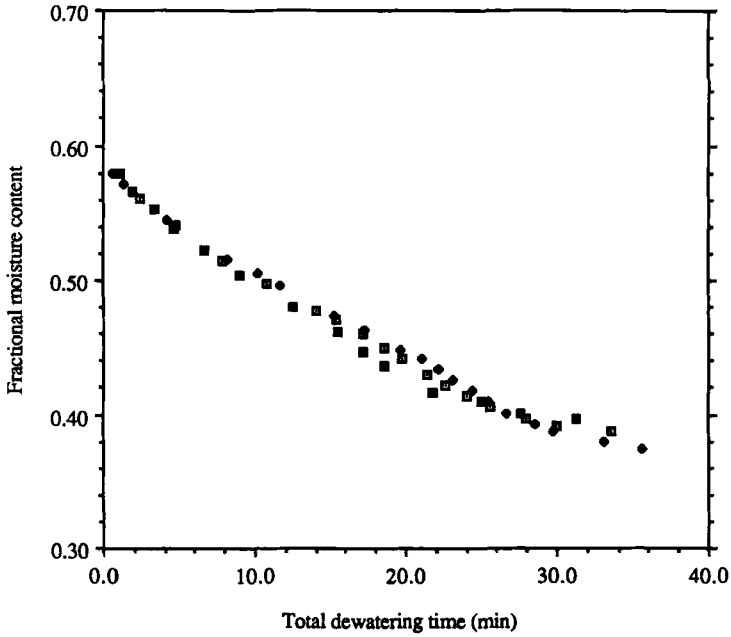

FIG. 1. Dewatering tests on untreated ochre slurry with an applied potential of 35 V. (□) Untreated, −35 V; (◆) untreated, +35 V; (■) untreated, 0 V.

Effects of Surfactant CTAB

Experiments were designed to investigate the effects of CTAB concentration on both the hydraulic and electrical dewatering behavior of ochre slurries at constant pressure and temperature. Figure 2 illustrates that for vacuum filtration only, when the concentration of CTAB is doubled, there is an enhancement in the rate and extent of hydraulic filtration. The addition of CTAB decreases the interfacial tension between the solid and the liquid, causing the value of the capillary pressure drop, ΔP_{cap}, to decrease. This will be discussed in more depth in the Discussion section.

At CTAB concentrations ranging from 5.6×10^{-4} to 2.0×10^{-3} M, the effect of an applied potential of 35 V with the bottom electrode positive indicates the absence of a significant change in the rate of water removal by electroosmosis (Fig. 3). However, it should be noted that there still appears to be a faster reduction in the fractional moisture content over time as the CTAB concentration is increased. This decrease is accompanied by an increase in the overall dewatering flow rate. When the polarity of the system is reversed (i.e., bottom electrode negative) at the same applied potential of 35 V, there is still the absence of an electroosmotic effect.

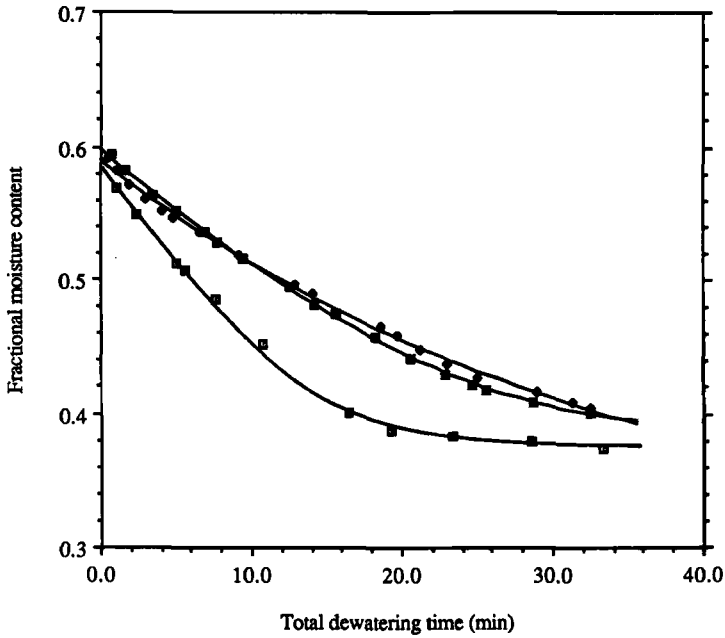

FIG. 2. Hydraulic dewatering (no applied potential) with varying CTAB concentration. (□) 1.1 E-3 M CTAB, 0 V; (♦) 5.2 E-4 M CTAB, 0 V; (■) 5.7 E-4 M CTAB, 0 V.

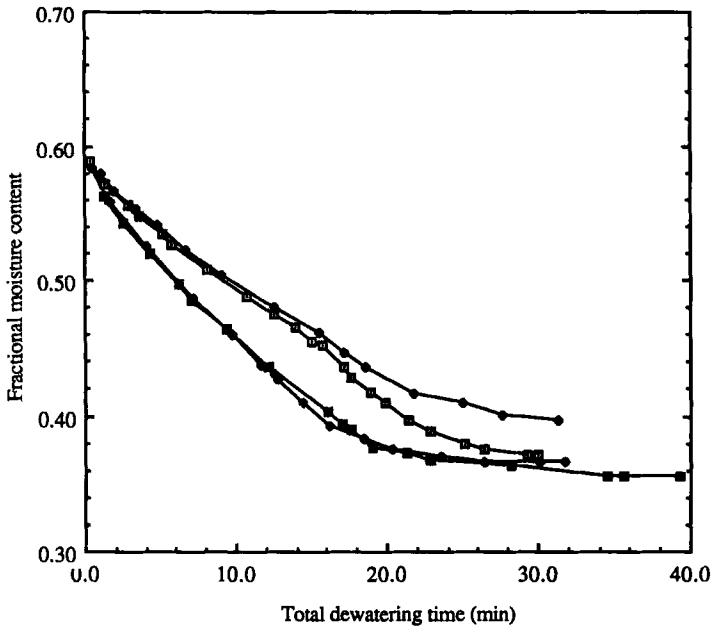

FIG. 3. Electroosmotic dewatering with CTAB only, effect of increasing concentration with an applied potential of +35 V. (□) 5.6 E-4 *M* CTAB, +35 V; (♦) 1.1 E-3 *M* CTAB, +35 V; (□) 2.0 E-3 *M* CTAB, +35 V; (◇, top curve) untreated slurry, 0 V.

Confirmation of the lack of charge on the ochre particles upon surfactant addition is provided by zeta-potential analysis. Electrophoretic measurements indicated a particle velocity of zero and consequently an electrophoretic mobility/zeta potential of zero, indicating that the ochre system is still at the point of zero charge.

Experimental Testing with Base Alone

Potential-determining ions control the surface charge and the potential at the surface of the dispersed phase. For iron oxides, the selective adsorption of OH^- and H^+ ions can be controlled by the addition of acids or bases (*9*). Oxide surfaces possess a large number of amphoteric hydroxyl groups that can react with either H^+ or OH^- as follows:

$$MOH_2^+ \xleftarrow{H^+} M{-}OH \xrightarrow{OH^-} M(OH)_2^- \qquad (2)$$

This reaction depends on the pH and may be termed as either an adsorption or a dissociation reaction.

The addition of sodium hydroxide has been determined by earlier studies

to generate an electroosmotic effect on iron oxide particles (*13*, *14*). In this study the addition of the base has a dual purpose: 1) it increases the pH of the system, with the corresponding zeta potential becoming increasingly negative, and 2) it provides sites for subsequent electrostatic adsorption of CTAB ions. An important relationship in electrokinetics is that between pH and zeta potential. In iron oxide the potential determining ions are H^+ and OH^-; an increase in pH provides more hydroxide ions which adsorb onto the surface of the ochre. Therefore, zeta potential is an indirect measurement of the extent of potential-determining ion adsorption.

A series of base alone tests were conducted with hydraulic dewatering as the sole driving force in order to observe the slurry dewaterability at various concentrations of sodium hydroxide. Figure 4 indicates that under the influence of vacuum alone, an increase in the NaOH concentration from 3.4×10^{-4} *M* to in excess of 9.9×10^{-3} *M* results in a significant decrease in the final moisture content in the system. As the base concentration increases, there is a corresponding decrease in the slope of the

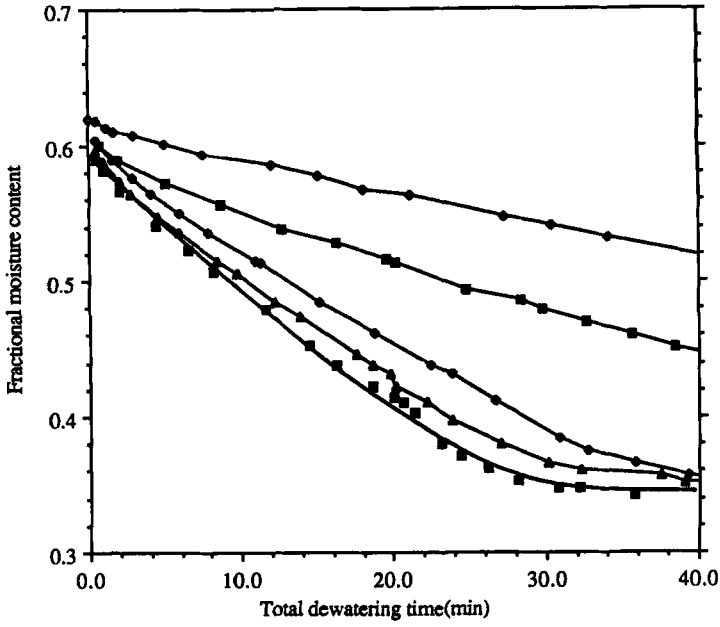

FIG. 4. Varying NaOH concentration (0 through 9.9 E-3 *M*) with vacuum dewatering only (no CTAB). (■, bottom curve) Untreated, 0 V; (△) 3.4 E-3 *M* base, 0 V; (◆) 5.3 E-3 *M* base, 0 V; (■, second curve from top) 7.3 E-3 *M* base, 0V; (◇) 9.9 E-3 *M* base, 0 V.

fractional moisture content versus time curves. In the base alone testing, this reduction in hydraulic dewaterability is attributed to the dispersal of the particles in the natural ochre due to the surface adsorption of hydroxide ions.

It becomes apparent that the vacuum-base alone mode of operation is unfeasible for two key reasons: 1) additional hydraulic energy and time must be expended to remove the excess water still present at a final dewatering time of t_{mod} = 20 min, and 2) the cost of sodium hydroxide (although a commodity chemical) is not offset by an increase in the extent of dewatering solely under hydraulic dewatering operation.

A demonstration of the performance of sodium-hydroxide-treated slurry under the conditions of electroosmotic dewatering is presented in Fig. 5. The observed electroosmotic effect is due to the presence of adsorbed hydroxide ions on the ochre surface. The hydroxide ions increase the concentration of potential-determining ions, generating a negatively charged surface. These base alone tests can be compared to the untreated ochre slurry which lacks the electrical capacity to produce an electroosmotic effect. Closer analysis of Fig. 5 demonstrates how the inhibition of hydraulic

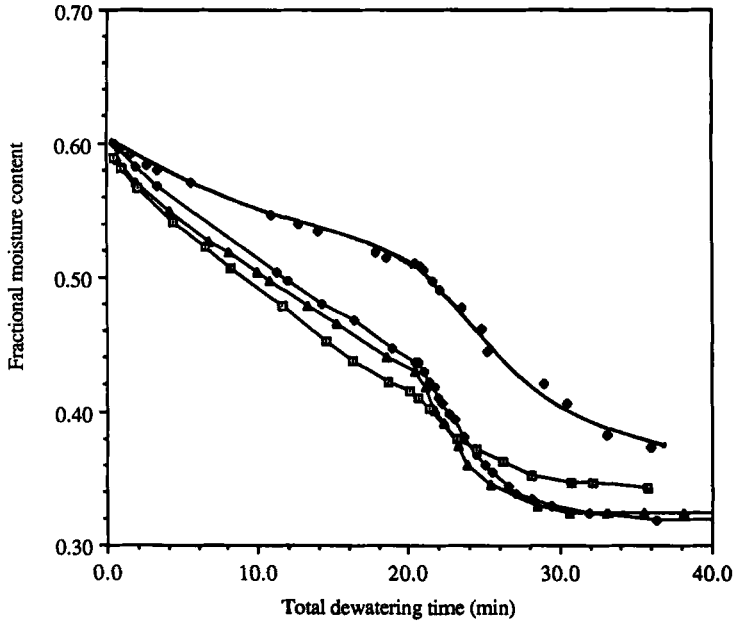

FIG. 5. Effect of varying NaOH (0 to 9.9 E-3 *M*) concentration on electroosmotic dewatering at an applied potential of −45 V. (□) Plain, 0 V; (△) 2.3 E-3 *M* base, −45 V; (◆) 5.3 E-3 *M* NaOH, −45 V; (◇) 7.2 E-3 *M* NaOH, −45 V.

flow with sodium hydroxide at concentrations of 2.3×10^{-3} and 5.5×10^{-3} *M* is overcome by an electroosmotic enhancement. For these two concentrations, the final moisture content of the NaOH treated slurry at $t_{mod} = 16$ min is lower than the final moisture content of the untreated slurry. However, at higher concentrations of base (7.2×10^{-3} *M*) the generation of an electroosmotically enhanced rate of liquid removal does not compensate for the hydraulic reduction in final moisture content produced when the slurry is treated solely with sodium hydroxide.

A study of the electrical properties of the ochre particles correlates well with the observed enhanced flow rates during electroosmotic dewatering. Rank microelectrophoretic studies of NaOH-treated slurries yield electrophoretic mobilities ranging from 1.2×10^{-8} to 3.3×10^{-8} $m^2/V \cdot s$ with corresponding zeta potentials of 15.4 to 42.3 mV (see Fig. 8). The relationship between zeta potential and NaOH concentration verifies the mechanism of hydroxide ion adsorption; the ochre particles become increasingly negative, corresponding to an increase in hydroxide-potential-determining ion concentration.

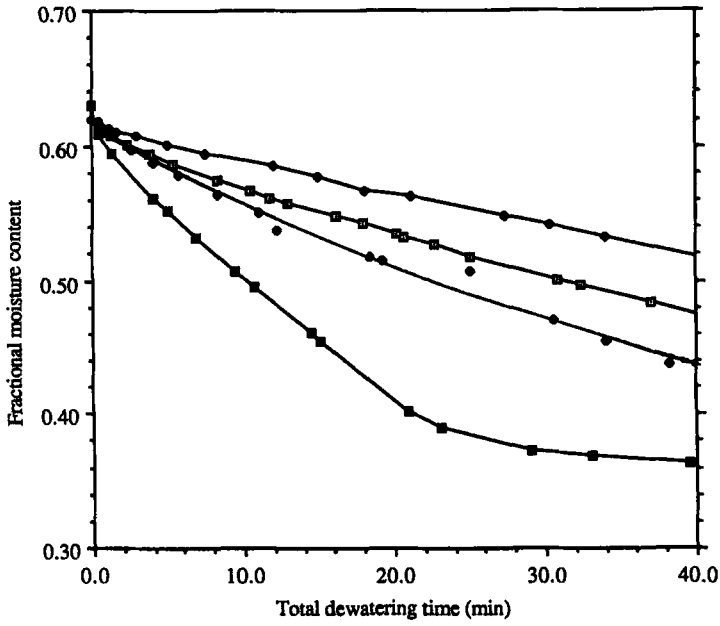

FIG. 6. Constant NaOH concentration of 9.8 E-3 *M* with a vacuum dewatering varying CTAB concentration from 9 E-3 *M* to 3 E-3 *M*. (◆) 0 *M* CTAB, 0 V; (□) 5.4 E-4 *M* CTAB, 0 V; (◇) 8.5 E-4 *M* CTAB, 0 V; (■) 3.0 E-3 *M* CTAB, 0 V.

Synergistic Effect of Base and Surfactant

At a given concentration of NaOH in the ochre slurry, increasing amounts of CTAB were added to the base-treated slurry; the relative contributions of electroosmotic and hydraulic dewatering to the overall filtration rates were determined. The CTAB concentration series was then repeated at different starting concentrations of NaOH in the ochre slurry. The purpose of CTAB addition following adsorption of hydroxide ions is twofold. First, the electrostatic adsorption of surfactant reduces the dispersing effect that base has on the slurry through reflocculation of the ochre particles. Second, the adsorption of a small quantity of CTA^+ ions permits the particle surface to retain enough charge from the hydroxide ion adsorption to generate an electroosmotic effect. An excess of either hydroxide ions or CTAB can have a detrimental effect on the rate and extent of dewatering.

The sodium hydroxide concentrations were 5×10^{-4}, 2.5×10^{-3}, 5×10^{-3}, 7×10^{-3}, and 9×10^{-3} *M*. At each NaOH concentration the following surfactant (CTAB) amounts were added to the dispersion: 0, 5 ×

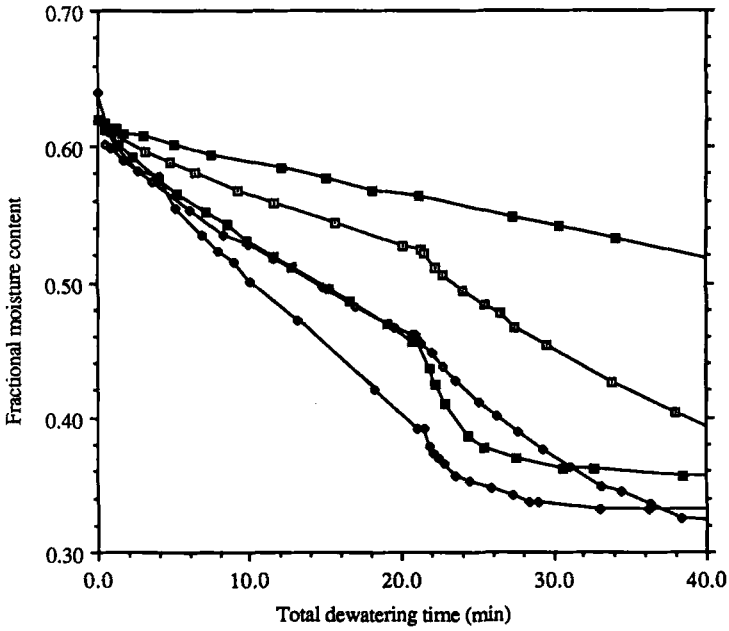

FIG. 7. ELectroosmotic dewatering at a NaOH concentration of 9.8 E-3 *M* with an applied potential of −45 V. (■, top curve) 0.0 *M* CTAB; (□) 5.2 E-4 *M* CTAB; (◇) 8.5 E-4 *M* CTAB; (■, second curve from bottom) 3.0 E-3 *M* CTAB; (◆) 4.8 E-3 *M* CTAB.

10^{-4}, 9×10^{-4}, 2.5×10^{-3}, and 5×10^{-3} *M*. The best condition for filtration necessitates a balance between the state of particle aggregation, which effects the hydraulic contribution, and the magnitude of the zeta potential, which determines the electroosmotic enhancement. An assessment of the concentration range of NaOH and CTAB which results in the best enhanced dewatering scheme is made by comparing dewatering performance between the elements in the concentration matrix.

At a NaOH concentration of 9×10^{-3} *M*, the highest base concentration used in this series, the CTAB concentration is increased from 5.2×10^{-4} *M* to a value of 4.8×10^{-3} *M*. When compared to untreated (or plain) slurry under vacuum alone conditions (Fig. 6), in the vacuum portion of the curves there is an increase in the rate and extent of dewatering as the concentration of CTAB is increased. Earlier tests indicate that a NaOH concentration of 9×10^{-3} *M* causes a significant decrease in the dewaterability of the slurry in the absence of surfactant. A comparison of this base alone test to one with a small amount of CTAB (5.4×10^{-4} *M*) supports the proposed adsorption mechanism which describes the reflocculation of base-dispersed particles through hydrophobic attraction of the adsorbed CTAB tails.

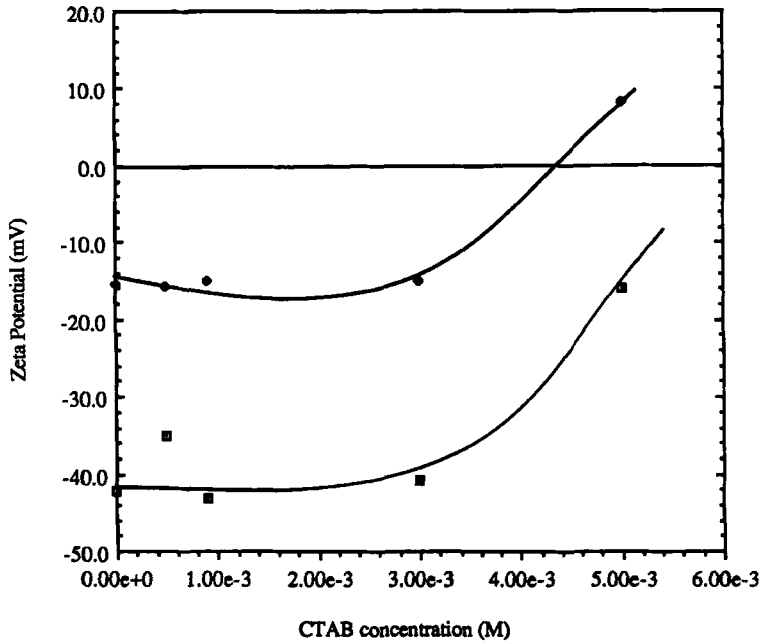

FIG. 8. Zeta potential values as a function of CTAB concentration with varying NaOH concentration. (□) 9 E-3 *M* NaOH; (♦) 9 E-4 *M* NaOH.

At a total dewatering time of 20 min, an applied potential of -45 V (Fig. 7) causes an electroosmotic enhancement in the entire CTAB concentration range at a constant NaOH concentration of 9.3×10^{-3} M. However, the rate of electroosmotic enhancement is not as pronounced at the lowest CTAB concentration (5.2×10^{-4} M). For the ochre slurry at 9.8×10^{-3} M NaOH, the lowest final fractional moisture content of 0.351 is achieved at a CTAB concentration of 3.0×10^{-3} M. In this system the combined electroosmotic improvement and high hydraulic permeability resulted in an optimal extent of dewatering conditions.

A series of plots of zeta potential against CTAB molarity are shown in Fig. 8 for increasing base concentration. There is no appreciable change in the zeta potential with increasing CTAB until the higher molarities (i.e., CTAB $> 3\times 10^{-3}$ M) are reached. The increase in slope over the entire range of surfactant concentration supports the mechanism of hydroxide adsorption in all cases. Further examination of the curves reveals that the highest CTAB concentration (5×10^{-3} M) exhibits the least negative value of zeta potential at both NaOH concentration values; the zeta potential also takes on a positive value at the lowest base concentration. This result supports the earlier mentioned theory of charge reversal with excess CTAB through multilayer adsorption.

DISCUSSION

Void Fraction

The void fraction is the fraction of the total cake volume available for transport of fluid. The void fraction of the growing solid cake is an important parameter in characterizing hydraulic flow of the filtrate. This property must be determined before we can estimate the specific surface cake resistivity and filter media resistance. Traditionally, the cake is weighed and then the superficial volume is measured, thus giving the cake density. If the specific gravity of the individual particles in the cake is known, then the porosity is represented as

$$\epsilon = 1 - \frac{\rho_{\text{cake}}}{\rho_{\text{particle}}} \tag{3}$$

The major shortcoming of this method is that the cake tends to consolidate after fluid has been moving through it for some time. There are further problems associated with obtaining exact weight and volume measurements.

A novel method, used in this study, to obtain cake porosity or void fraction takes advantage of the electrical network already in place for the

electroosmotic study. In electroosmotic separation, the current–voltage relationship for a single capillary, along the length of the capillary, L, is

$$i = \frac{\Phi}{L} \pi a^2 K \tag{4}$$

where a is the capillary radius, K is the liquid conductivity, and Φ is the total potential drop (*15*). The value of K may be determined independently for each filtrate sample by using information from the electrophoretic mobility measurements. In the microelectrophoretic apparatus the capillary radius and length are known, the current is measured for a given voltage, and Eq. (4) is used to calculate K.

In the case of a porous cake, the cross-sectional area of the cake available for flow (A_T) must be accounted for by multiplying the total cross-sectional area by the void fraction so that

$$i = \frac{\Phi}{L} K \epsilon A_T \tag{5}$$

The porosity may be represented as

$$\epsilon = \frac{iL}{\Phi K A_T} \tag{6}$$

For electroosmotic dewatering, if the current flow is measured for a given potential drop across the cake, we may ascertain the value of ϵ at any time during the application of voltage, as long as L and i are measured.

Cake and Filter Resistivity

Specific resistance is a technique implemented to study the hydraulic filterability of the ochre as a function of varying additive concentrations. Specific resistance calculations were performed on the volume–time dewatering data obtained in this study by using the method described in Geankopolis (*16*). To determine the cake and filter characteristics for the case of a growing cake, Eq. (7) can be used to describe the relationship of the filter medium, volume flow rate, and pressure drop during filtration:

$$Q_{vac} = \frac{dV}{dt} = \frac{\Delta P_T A_T}{\mu \left(\frac{\alpha C_s V}{A_T} + R_m \right)} \tag{7}$$

where R_m is the filter medium resistance, C_s is the concentration of solids in the slurry, μ is the viscosity of the filtrate, and V is the volume of liquid removed in time t. The actual total pressure drop in the system, ΔP_T, is

$$-\Delta P_T = -\left(\Delta P_m - \frac{2\sigma \cos \theta}{a}\right) \tag{8}$$

where ΔP_m is the measured pressure drop. The specific resistance, α, is defined as

$$\alpha = \frac{k_1(1 - \epsilon)S_0^2}{\rho_p \epsilon^3} \tag{9}$$

where k_1 is a constant and equals 4.17 for random particles of definite shape and size, σ is the interfacial tension, and θ is the solid/liquid contact angle in degrees.

The specific surface of the particles, S_0, is defined by

$$S_0 = 6/\phi D_p \tag{10}$$

where ϕ is the particle shape factor and D_p is the mean particle size. The filter constant R_m may vary from one filter to another and has the units of inverse meters.

To evaluate α and R_m, we invert Eq. (7):

$$dt/dV = K_p V + B \tag{11}$$

where

$$K_p = \frac{\mu \alpha C_s V}{\Delta P_T A_T^2} \quad \text{and} \quad B = \frac{\mu R_m}{\Delta P_T A_T} \tag{12a,b}$$

Using the data of volume collected, V, at time t during a test, we take differences at successive intervals and plot $\Delta t/\Delta V$ versus V', where V' is the average volume of liquid collected within the time interval Δt. The slope of the line is K_p and the intercept is B.

Although the values of K_p and B are available, the value of ΔP_T is unknown. For this reason, α and R_m may not be directly calculated. In addition, for a growing cake the specific surface area of the solid material in the cake is unknown. Although it is possible to measure the size and shape of individual particles of the slurry prior to dewatering, in this re-

search the particles are subject to agglomeration and consolidation during cake formation. Hence, an independent determination of particle size would not provide an accurate indication of the specific surface area of the cake matrix. An approximation method is used here to avoid the difficulty stated above. As the cake grows, there are two major resistances to filtrate flow: one in the cake,

$$Q_c = \frac{-\Delta P_c A_T}{\mu \alpha C_S V} \tag{13}$$

and one in the filter medium,

$$Q_m = \frac{-\Delta P_f A_T}{\mu R_m} \tag{14}$$

where ΔP_c is the pressure drop across the cake and ΔP_f is the pressure drop across the filter medium. In the above method, the two resistances are combined to solve for α and R_m.

The total actual pressure drop (ΔP_T) may be represented as the sum of the resistances to flow through the cake and the medium. The value of ΔP_T may also be represented as the difference between the measured pressure drop (ΔP_m) and the pressure reduction due to capillarity in the cake (ΔP_{cap}):

$$\Delta P_T = \Delta P_m - \Delta P_{cap} = \Delta P_c + \Delta P_f \tag{15}$$

the capillary pressure drop in the bed may be represented as

$$\Delta P_{cap} = \frac{2\sigma \cos \theta}{a} \tag{16}$$

where σ is the surface tension, a is the capillary radius, and θ is the contact angle between the liquid and the solid. The problem here is that the total actual pressure drop in the system, ΔP_T, is unknown due to the capillary pressure also being an unknown. We can solve independently for the value of R_m by estimating the flow rate at the beginning of the dewatering run ($t = 0$). Early in the filtration process, before the cake has had a chance to form, most of the resistance to flow is in the filter medium:

$$Q_{t=0} = \frac{-\Delta P_f A_T}{\mu R_m} \tag{17}$$

and therefore

$$R_m = \frac{-\Delta P_f A_T}{Q_{t=0}\mu} \tag{18}$$

In this analysis, it is assumed that the capillary pressure drop in the filter medium is negligible. By extrapolating the flow rate data to a very low value of time, the value of R_m may be determined by using ΔP_f as the total applied pressure.

For the case of the growing cake, by using the graphically determined values of K_p and B with the calculated value of R_m from initial flow rates, the following relationship is developed:

$$\frac{\alpha}{R_m} = \frac{K_p}{B}\frac{A_T}{C_s} \tag{19}$$

From this equation the specific resistance, α, may be calculated. Electroosmotic measurements provided the value of ϵ, which in turn is used to find the specific surface area by using the following equation:

$$S_0 = \left(\frac{\alpha\rho_p\epsilon^3}{k_1(1-\epsilon)}\right)^{1/2} \tag{20}$$

The results of the specific surface area, porosity, specific resistance, and estimated pore size for the range of concentrations of NaOH and CTAB are presented in Table 1.

The value of K_p is dependent on both the cake pore size, a, and the contact angle, θ, both unknown quantities; as part of ΔP_T, it is necessary to find K_p for a case where the contact angle is known or can be reasonably estimated. As a first approximation, those tests where the CTAB concen-

TABLE 1
Relationship between NaOH Concentration and Specific Resistance Parameters

NaOH concentration (M)	ϵ	$S_0 \times 10^{-6}$ (m^{-1})	$\alpha \times 10^{-11}$ (mkg^{-1})	$a \times 10^6$ (m^{-1})	$N \times 10^{-7}$
9.0×10^{4}	0.40	7.67	6.57	4.12	4.77
2.5×10^{-3}	0.42	7.26	4.78	4.01	5.33
5.0×10^{-3}	0.44	8.00	4.84	4.27	4.93
7.0×10^{-3}	0.53	8.14	2.56	3.62	8.14
9.0×10^{-3}	0.52	9.29	3.46	3.74	7.56

tration was the greatest, and the surface tension the lowest, were taken as representative of the situation for which $\theta = 0$ and $\cos\theta = 1.0$. This allowed us to estimate a value for the pore radius for a series of tests conducted at a constant NaOH concentration.

For the other tests in the series, at lower CTAB concentrations, and using the same value of a already found, the value of $\cos\theta$ and hence θ could be found for each successive test (see Table 2). This analysis indicates that although the void fraction generally increases with NaOH concentration, the pore size and particle size (inverse of specific surface) decrease. This suggests that the adsorption of hydroxide ions tends to create a greater number of fine particles which produce finer pores. The total number of pores in the filter cake is found from

$$N = A_T\epsilon/\pi a^2 \tag{21}$$

The value of N ranges from 4×10^7 to 10^8 over the range of increasing hydroxide ion concentration (see Table 1). A plausible explanation for this

TABLE 2
Estimated Contact Angle and Medium Resistance as a Function of CTAB and NaOH Concentration (M)

	CTAB concentration				
NaOH concentration	0.0	5×10^{-4}	9×10^{-4}	2.5×10^{-3}	5×10^{-3}
9×10^{-4}					
θ	54.2	40.6	39.1	2.63	0.0
$R_m \times 10^{-11}$	6.30	7.97	3.00	3.99	2.50
2.5×10^{-3}					
θ	51.6	40.2	36.8	8.60	0.0
$R_m \times 10^{-11}$	5.25	3.72	3.26	6.90	1.81
5×10^{-3}					
θ	48.6	36.1	33.3	0.0	0.0
$R_m \times 10^{-11}$	1.22	6.03	3.76	4.33	5.28
7×10^{-3}					
θ	46.6	35.2	30.9	0.0	0.0
$R_m \times 10^{-11}$	5.21	2.83	3.04	4.02	2.57
9×10^{-3}					
θ	—	32.3	32.8	0.0	0.0
$R_m \times 10^{-11}$	—	5.92	1.78	3.56	2.26

increase in the number of pores may be that, at lower base concentrations, the individual particles form larger flocs since they have lower zeta potential. These larger flocs result in a cake that consists of less uniform and larger pores, with a lower associated porosity. As the base concentration is increased, the particles settling into the cake are more dispersed and uniform, yielding a finer pore size with a larger overall porosity. This explanation verifies the proposed mechanism of OH^- and CTA^+ ion adsorption and the resulting flocculation. In addition, it is consistent with experimental observation of both dewaterability and zeta potential.

Average estimated contact angles increase from a value of zero for CTAB concentrations of 5×10^{-3} and 2.5×10^{-3} M to 50.3° for the case of zero CTAB. This can be compared with a value of 47° for water on silica (*17*). The reduction in surface tension along with the contact angle, by increasing the CTAB concentration, acts to enhance the vacuum dewaterability of the ochre. The vacuum dewatering efficiency may be expressed in terms of capillary pressure reduction:

$$E_{\text{vac}} = \frac{\Delta P_m - \dfrac{2\sigma \cos \theta}{a}}{\Delta P_m} \tag{22}$$

In Fig. 9 the vacuum dewatering efficiency, E_{vac}, is plotted versus CTAB surface tension to show the effect of reduction of capillary pressure. Although the CTAB addition shows a definite benefit in terms of hydraulic dewatering, this is negated by the addition of base, with a reduction in efficiency of over twofold in going from a base concentration of 9×10^{-4} to 9×10^{-3} M. The best combination of base and surfactant with respect to vacuum dewatering efficiency appears to be at the lower NaOH concentrations and highest CTAB concentration.

Determining the Electroosmotic Flow Rate from Experimental Data

The combined vacuum and electroosmotic flow rates have been measured at $t_{\text{mod}} = 0$ and for several minutes thereafter. In order to determine a value for Q_{eo}, we need to select a time for which we have data from the vacuum portion to subtract from the combined flow rate value, Q_{tot}, yielding the electroosmotic flow. To do this we plot the filtrate volume versus time and find the slope of this curve at $t_{\text{mod}} = 0$. Then we use the information gathered on vacuum dewatering to determine what this rate would be at $t_{\text{mod}} = 0$.

Generally, the addition of electroosmotic flow more than doubles the

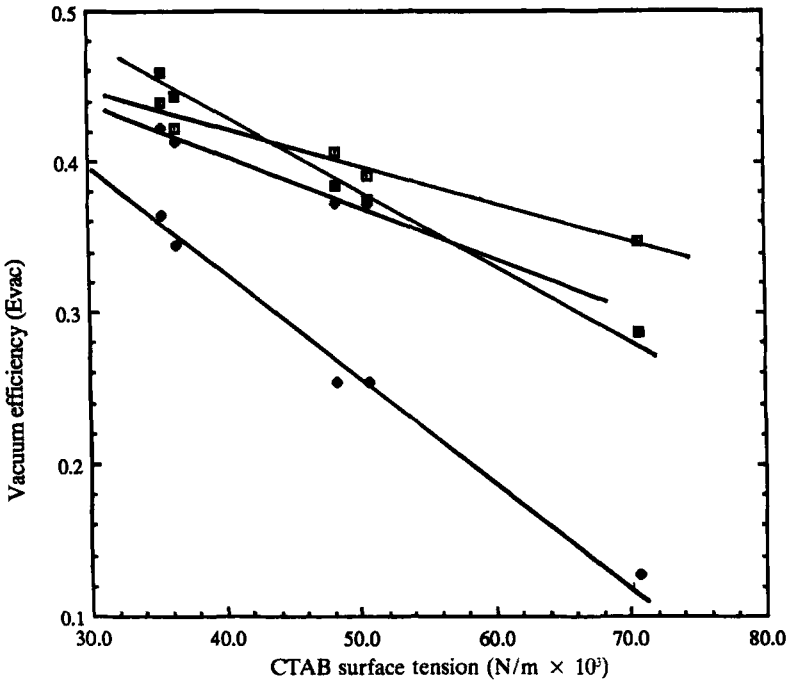

FIG. 9. Vacuum efficiencies over a range of NaOH concentrations as a function of CTAB surface tension. (□) 9 E-4 *M* NaOH; (♦) 2.5 E-3 *M* NaOH; (■) 5 E-3 *M* NaOH; (◇) 7 E-3 *M* NaOH.

flow solely under vacuum conditions. The addition of OH^- ions improves the flow rate by slightly over 50% in the concentration range of 9×10^{-4} to 9×10^{-3} *M*. We shall see in the next section that the amount of electrical energy expended may mitigate the overall benefits of electroosmotically enhanced flow.

The Electroosmotic Efficiency

An electroosmotic efficiency may be defined based on the amount of electrical energy put into the system. This is the fraction of electrical energy which is actually used to drive the fluid out of the slurry relative to the total energy input. We may determine from experimental results a value of the electroosmotic flow rate at the beginning of the electroosmotic portion of the run $Q_{eo_{t_{mod}=0}}$ by

$$Q_{eo_{t_{mod}=0}} = Q_{tot_{t_{mod}=0}} - Q_{vac_{t_{mod}=0}} \tag{23}$$

The experimental value is compared with the theoretical value:

$$Q_{eo} = \frac{\Phi \zeta \epsilon A_T}{L\mu} \tag{24}$$

where all of the parameters in this equation are known at $t = 0$, independently. Taking into account the surface conductance, the apparent cake thickness $(L + L_R)$ will be experimentally larger than the actual measured value of the cake thickness, L. Incorporation of the surface conduction effects in the actual conductivity term yields

$$K + \frac{2K_s}{a} \tag{25}$$

so we assume the ratio of length to conductivity in the porosity equation to be

$$\frac{L}{K} = \frac{L + L_R}{\left(K + \frac{2K_s}{a}\right)} \tag{26}$$

or

$$\frac{L_R}{L} = \frac{2K_s}{aK} \tag{27}$$

Making the above correction for surface conductance, the equation may be represented as

$$Q_{eo,exp} = \frac{i\zeta}{\left(K + \frac{2K_s}{a}\right)\mu} = \frac{\Phi \zeta \epsilon A_T}{(L + L_R)\mu} \tag{28}$$

where K_s is surface conductivity and a is the pore radius. The electroosmotic efficiency, E_{eo}, will be defined as

$$E_{eo} = \frac{L}{L + L_R} = \frac{K}{K + \frac{2K_s}{a}} \tag{29}$$

The value of L is known from the measured values of filtrate volume at

the beginning and the end of application of electrical energy by using

$$V = V_f - V_i = L\epsilon_0 A_T \tag{30}$$

The value of $L + L_R$ is found from

$$L + L_R = \frac{\Phi\zeta\epsilon A_T}{\mu(Q_{eo,exp})} \tag{31}$$

Figure 10 shows how average values of K_s and E_{eo} vary with CTAB surface tension. As the concentration of CTAB is increased, the surface tension is decreased, allowing more water to be removed hydraulically. However, this increase has a negative effect on the electroosmotic efficiency because it increases the surface conductivity, thus "short circuiting" much of the electrical energy.

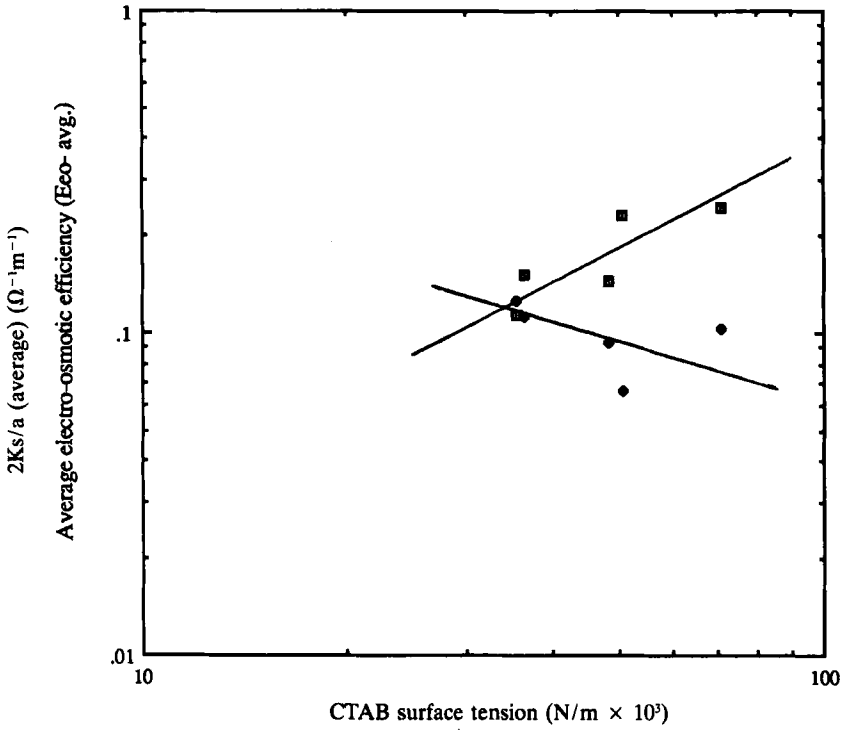

FIG. 10. Average electroosmotic efficiency as a function of CTAB surface tension. (□) E_{eo} (av); (◆) $2K_s/a$ (av).

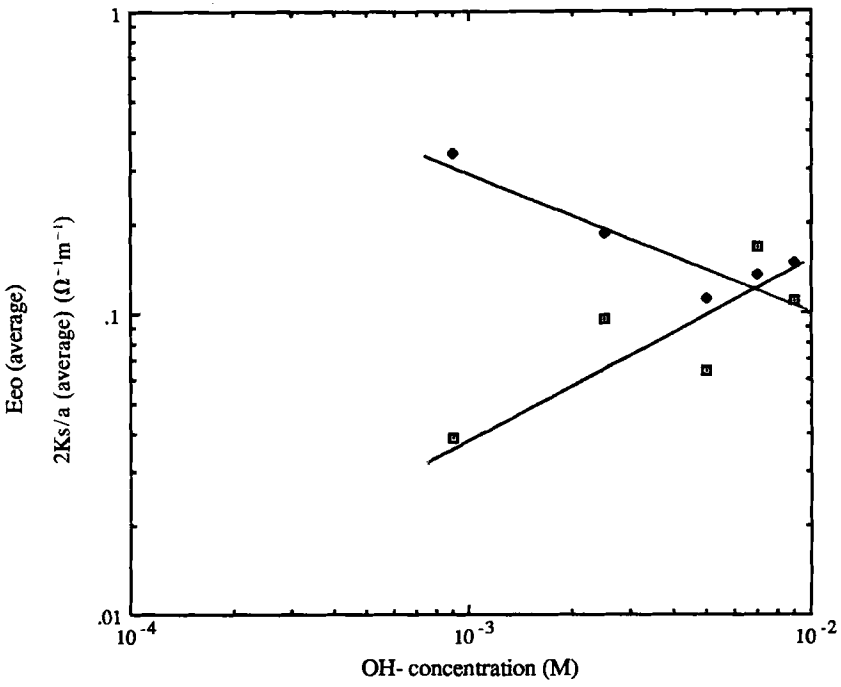

FIG. 11. Effect of increasing NaOH concentration on electroosmotic efficiency and surface conductance. (□) $2K_s/a$ (av); (♦) E_{eo} (av).

The experimental values for surface conductivity are high when compared to literature values. For example, for monolayers of stearic acid in distilled water, the K_s is 3.5–3.8 × 10^{-8} Ω^{-1} (*15*). However, the amount of CTAB applied may indeed provide the surface conductibility experienced in this research, especially if it is considered that the ochre sample may already possess high conductivity as evidenced by the K_s value at zero CTAB concentration ($K_s \approx 7 \times 10^{-8}\ \Omega^{-1}$).

In Fig. 11 we see how the average surface conductivity also increases with NaOH concentration, and that also acts to reduce the electroosmotic efficiency until the sodium hydroxide concentration is equal to 5 × 10^{-3} *M*, after which there is a slight rise. This may be a result of the rising zeta potential overcoming losses in conductivity.

CONCLUSIONS

The presence of ultrafine particles in slurries restricts the use of the hydraulic dewatering techniques due to a reduction in the size of the pores

in the filter cake. Electroosmotic dewatering is a process that can be implemented in conjunction with conventional methods of dewatering to significantly enhance the extent and rate of dewatering. A theoretical analysis of the experimental data supports the proposed adsorption–dewatering mechanism. Relationships were developed between filter cake porosity, specific resistance, and conductivity to separate the effects of CTAB and NaOH on the hydraulic and electroosmotic dewatering performance.

The untreated ochre slurry tested in this research exhibited no significant electroosmotic effect in the natural state; measured zeta potentials for the untreated slurry were zero, confirming the absence of an electroosmotic driving force. In tests conducted with CTAB alone, there was a slight increase in the rate and extent of hydraulic dewatering with increasing CTAB concentration. The reduction in surface tension produced by the addition of surfactant corresponded to an overall decrease in the capillary pressure drop.

The adsorption of hydroxide ions through the addition of NaOH to produce a surface charge on the particles causes dispersal, thereby inhibiting hydraulic flow rates. In the absence of CTAB, an increase in the NaOH from 9×10^{-4} to 7×10^{-3} M had an associated porosity increase from 0.40 to 0.53 and an estimated cake pore size decrease from 4.12×10^{-6} to 3.62×10^{-6} m, respectively. The reduction of the hydraulic permeability of the ochre slurry upon OH^- addition may be expressed by the reduction in vacuum dewatering efficiency (E_{vac}) from 0.348 to 0.127 over a NaOH range of 9×10^{-4} to 7×10^{-3} M.

An increase in the OH^- potential determining ion concentration causes an increase in the zeta potential of the iron oxide to enhance the rate of electroosmotic dewatering. In the absence of CTAB the measured zeta potential values increased from zero for the untreated slurry to -42.1 mV at a NaOH concentration of 9×10^{-3} M.

The addition of excess hydroxide ions results in unwanted dispersion of the ochre particles. Subsequent use of a flocculant in the form of CTAB will assist in the hydraulic dewatering of the slurry by flocculating the dispersion. The addition of an excess of CTAB can dampen the effects of the hydroxide ions through electrostatic adsorption of CTA^+ ions, reducing the electroosmotic enhancement. However, continued increases in CTAB concentration may result in charge reversal through the mechanism of multilayer adsorption. The use of both NaOH and CTAB as surface conditioning agents produces a synergistic reduction in the final cake moisture content in electroosmotic dewatering. An increase in the CTAB concentration from 0 to 5×10^{-3} M corresponds to an increase in the vacuum dewatering efficiency (E_{vac}) from 0.127 to 0.365 when the NaOH concentration is 7×10^{-3} M.

Extension of surfactant-enhanced electroosmotic dewatering to other fine particle systems requires an evaluation of the electrical and hydraulic parameters (e.g., zeta potential, specific resistance). An understanding of the interdependence of these two properties with chemical addition will be useful in the development of dewatering schemes for other uncharged fine particle systems. The predication of electroosmotic dewatering behavior should be applied with caution to impure fine particle systems or mixtures. The presence of other species could invalidate the predicted electrokinetic behavior by altering the surface conductivity and the zeta potential.

In summary, the following criteria exist for implementing chemically enhanced electroosmotic dewatering for an uncharged system (i.e., dispersion, slurry) within an existing industrial process: 1) a chemical additive must be selected that will impart sufficient zeta potential to the particles in small quantities, 2) the additive should be chemically compatible with other chemical species in the system and avoid the dispersion of particles, and 3) the integrity of the final product should be maintained (e.g., color and composition).

Acknowledgments

The authors wish to acknowledge support of this project by the Bureau of Mines, U.S. Department of the Interior, Allotment Grant #G1194113. The contents do not necessarily reflect the views and policies of the U.S. Bureau of Mines. Mention of commercially produced instruments and products does not constitute endorsement or recommendation for use by the U.S. Bureau of Mines.

REFERENCES

1. J. G. Sunderland, "Electrokinetic Dewatering and Thickening: I. Introduction and Historical Review of Electrokinetic Applications," *J. Appl. Electrochem., 17,* 889–898 (1987).
2. N. C. Lockhart, "Electro-osmotic Dewatering of Fine Tailings from Mineral Processing," *Int. J. Miner. Process., 10,* 131–140 (1983).
3. D. J. Kelsh and R. H. Sprute, "Water Removal from Mine Slimes and Sludge Using Direct Current," *Drying Technol., 1,* 57–81 (1984).
4. R. H. Sprute and D. J. Kelsh, "Electrokinetic Densification of Solids in a Coal Mine Sediment Pond—A Feasibility Study," *U.S., Bur. Mines, Rep. Invest., 8666* (1982).
5. J. Greyson, "Electroosmotic Sewage Sludge Dewatering," *Yale Sci. Mag., 44,* 6–10 (1970).
6. H. Yukawa, H. Yoshida, K. Kobayashi, and M. Hakoda, "Electroosmotic Dewatering of Sludge under Condition of Constant Voltage," *J. Chem. Eng. Jpn., 11,* 475–480 (1978).
7. D. Ellis and J. G. Sunderland, *Dewatering Sewage Sludge by Electro-Osmosis. Part II. Scale-Up Data,* NTIS Report PB-276 412, 1977.
8. D. J. Shaw, *Electrophoresis,* Academic, London, 1969.

9. R. J. Hunter, *Zeta Potential in Colloid Science: Principles and Applications,* Academic, London, 1981.
10. Z. Keesom and Radke, "A Zeta Potential Model for Ionic Surfactant Adsorption on an Ionogenic Hydrophobic Surface," *J. Colloid Interface Sci., 125,* 575–585 (1988).
11. D. P. Mickelsen, "Iron Oxide Pigments," in *Bureau of Mines Minerals Yearbook,* 1985, pp. 541–551.
12. I. Iwasaki, S. R. B. Cooke, and H. S. Choi, "Flotation Characteristics of Hematite, Goethite and Activated Quartz," *Am. Inst. Min. Met. Pet. Eng. Trans., 217,* 237–244 (1960).
13. C. S. Grant and E. J. Clayfield, "Surfactant Enhanced Electro-osmotic Dewatering in Mineral Processing," in *Interfacial Phenomena in Biotechnology and Materials Processing Proceedings* (Y. A. Attia, B. M. Moudgil, and S. Chander, eds.), Elsevier Science, Amsterdam, 1988.
14. C. S. Grant, "Surfactant Enhanced Electro-osmotic Dewatering of Mineral Ultrafines," Doctoral Dissertation, Georgia Institute of Technology, Atlanta, Georgia, 1989.
15. J. T. Davies and E. K. Rideal, *Interfacial Phenomena,* Academic, New York, 1963.
16. C. J. Geankopolis, *Transport Processes and Unit Operations,* 2nd ed., Allyn and Bacon, Boston, 1983.
17. S. Ross and I. D. Morrison, *Colloidal Systems and Interfaces,* Wiley-Interscience, New York, 1988.

Received by editor June 21, 1990